RGG1, involved in the cytokinin regulatory pathway, controls grain size in rice

Yajun Tao
Jiangsu Academy of Agricultural Sciences https://orcid.org/0000-0002-4810-0225
Jun Miao
Yangzhou University
Jun Wang
Jiangsu Academy of Agricultural Sciences
Wenqi Li
Jilin Academy of Agricultural Sciences
Yang Xu
Jiangsu Academy of Agricultural Sciences
Fangquan Wang
Jiangsu Academy of Agricultural Sciences
Yanjie Jiang
Jiangsu Academy of Agricultural Sciences
Zhihui Chen
Jiangsu Academy of Agricultural Sciences
Fangjun Fan
Jiangsu Academy of Agricultural Sciences
Mengbin Xu
Yangzhou University
Yong Zhou
Yangzhou University
Guohua Liang
Yangzhou university
Jie Yang (yangjie168@aliyun.com)
Jiangsu Academy of Agricultural Sciences

Original article

Keywords: heterotrimeric G protein, RGG1, rice, grain size, cytokinin

Posted Date: July 8th, 2020

DOI: https://doi.org/10.21203/rs.3.rs-40598/v1

Version of Record: A version of this preprint was published on November 10th, 2020. See the published version at https://doi.org/10.1186/s12284-020-00436-x.

Abstract

Heterotrimeric GTP binding proteins (G proteins) and cytokinin play important roles in regulating plant growth and development. However, little is known about the mechanism by which they coordinate the regulation of grain size in rice. We functionally characterized one gene, *RGG1*, encoding a type-A Gγ subunit. Strong GUS staining were detected in young panicles and spikelets, suggesting the role of this gene in modulating panicle-related traits development. By regulating cell division, over-expression of *RGG1* in Nipponbare (NIP) and Wuyunjing 30 (WYJ30) significantly decreased plant height, panicle length and grain length. However, *rgg1* mutants generated by CRISPR/Cas9 system exhibited no obvious phenotypic differences, which may be due to its extremely low expression level in vivo. Transcriptomic analysis showed that differentially expressed genes (DEGs) were enriched in the cytokinin biosynthesis pathway. We confirmed this result by measuring the endogenous cytokinin levels and showed that the content of cytokinin was lower in OE lines. Additionally, the results of 6-benzylaminopurine (6-BA) treatment showed that increased expression of *RGG1* decreased the sensitivity to 6-BA under low concentration. Our results reveal a novel G proteins—cytokinin module controlling grain size in rice, which will be beneficial for understanding the mechanisms of G proteins regulating grain size and plant development.

Background

Heterotrimeric GTP binding proteins (G proteins) are key regulators of a multitude of transmembrane signaling pathways in animals and plants. The heterotrimeric protein complex is composed by Gα, Gβ, and Gγ subunits, which circularly swap between active and inactive forms. G protein signaling is activated by seven-pass trans-membrane G protein–coupled receptors (GPCRs) that function as guanine nucleotide exchange factors and then transduce the signal to downstream effectors (Pandey 2019). In plants, G proteins are involved in multiple fundamental growth and development pathways, including panicle branching (Huang et al., 2009; Zhou et al., 2009), seed size (Liu et al., 2018; Mao et al., 2010; Sun et al., 2018), shoot apical meristem (SAM) development (Bommert et al., 2013), nitrogen utilization (Sun et al., 2014), and stress tolerance (Yu and Assmann 2015; Zhang et al., 2015).

Although G proteins are evolutionarily conserved, their number varies widely between human and plants. For example, there are at least 23 Gα, 5 Gβ and 12 Gγ identified in humans. In contrast, the genomes of rice have only one Gα (*RGA1*), one Gβ (*RGB1*), and five Gγ homologs (*RGG1*, *RGG2*, *GS3*, *qPE9-1*/*DEP1*, and *GGC2*) (Sun et al., 2018). The mutation of *RGA1* caused a severe dwarf and small grains (Zong et al., 2018). Additionally, *RGA1* is also involved in regulating rice gibbering and brassinosteroids signaling (Ueguchi-Tanaka et al., 2000; Wang et al., 2006). The Gβ gene, *RGB1*, positively regulates cellular proliferation to modulate internode elongation and grain size (Utsunomiya et al., 2011). Evidence also shows that *RGB1* functions as a positive regulator of ABA to modulate rice drought tolerance (Zhang et al., 2015). The five Gγ proteins antagonistically regulate grain length in rice. In particular, GS3, qPE9-1/DEP1, and GGC2 competitively interact with Gβ to control grain size (Sun et al., 2018). qPE9-1/DEP1 could directly interact with MADS-domain transcriptional factor OsMADS1 and enhance its

transcriptional activity to control grain size (Liu et al., 2018). *RGG2*, encoding a type B Gβ subunit, negatively regulates grain size and also involved in gibberellin signaling (Miao et al., 2019). These prior studies in rice reveal that G proteins play a vital role in determination of grain size as well as in phytohormone regulation.

Phytohormone plays diverse roles in plant growth and development (Blázquez et al., 2020). Cytokinin, one of the most important phytohormone, has been shown to modulate panicle traits. *Gn1a* encodes a cytokinin oxidase/dehydrogenase enzyme, that is responsible for cytokinin degradation in vivo. Mutation in *Gn1a* results in accumulation of cytokinin and cause an increase in grain number per panicle (Ashikari et al., 2005). Conversely, the cytokinin-activating enzyme, LOG, directly converts inactive cytokinin to biologically active forms. The *log* mutant has highly reduced SAMs and panicles, and abnormal branching patterns (Kurakawa et al., 2007). Cytokinin signaling pathway plays important roles in regulating meristem cells proliferation and differentiation (Stahl and Simon 2010). There were studies shown G proteins are also involved in stem cell fate determination. Maize *COMPACT PLANT2* (*CT2*), coding a G protein Gα subunit, interacts with FASCIATE EAR2 (CLV2) to regulate inflorescence meristem size (Bommert et al., 2013). In *Arabidopsis*, the mutants of Gβ showed an enlarged meristem size (Ishida et al., 2014). AGB1 interacts with RPK2, one of the CLV3 peptide hormone receptors, to regulate meristem development. However, rice G proteins involved in CLAVATA signaling have not been reported.

Decreased levels of cytokinin also lead to reduced grain size in the *root enhancer1* (*ren1-D*) mutant due to activation of *OsCKX4* (Gao et al., 2014), and grain size may be regulated in part by modulation of long-distance transport of cytokinin by *Big Grain3* (*BG3*), which encodes a purine permease, *OsPUP4* (Xiao et al., 2019). Recently, the Gγ subunit, *qPE9-1/ DEP1*, was found to positively regulate grain-filling by increasing endogenous cytokinin and auxin concentrations in rice grains (Zhang et al., 2019). However, how G proteins interact with cytokinins to control growth and development in plants remains largely unknown.

In this study, we functional analyzed the γ subunit gene *RGG1* in rice. Overexpression of *RGG1* caused reduced plant height and grain length. Further results suggested that *RGG1* modulates endogenous cytokinin accumulation and response to regulate plant morphology and grain development.

Results

RGG1 encodes a type A Gγ subunit

In the rice genome, five Gγ subunits have been identified. Among them, RGG1 is relative small and contains four exons (Fig. 1a). Phylogenetic analysis showed that G proteins of rice, *Arabidopsis*, and maize were divided into three groups (Fig. 1b). Among types A, B and C, amino acid sequences showed very little conservation, and most of the similarities are limited to a highly conserved GGL (G gamma-like) domain (Fig. S1). *RGG1* is located in a clade of type A G proteins along with the *AGG1* and *AGG2* proteins of *Arabidopsis*. SMART analysis predicts that *RGG1* contains a nuclear location signal (NLS) at the N-

terminus, a GGL domain, and a CaaX isoprenylation motif at C-terminal end, typical of all canonical type A G proteins (Fig. S1).

We confirmed that RGG1 interacts with RGB1 using a BiFC assay. The fluorescence signal of BiFC were detected in membrane, cytoplasm and nucleus suggesting the potential function of the Gβγ dimer (Fig. 1c). To further explore the interacting site of RGG1 and RGB1, several truncated RGG1 proteins were generated. As shown in Figure 1d, GGL domain was necessary and sufficient for the interaction with RGB1. In addition, the 55-67 residues of RGG1 was required for the RGG1-RGB1 interaction (Fig. 1d).

Expression profiles and subcellular location

To determine the expression pattern of RGG1, the tissue specific expression of *RGG1* was detected using transgenic plants containing a *RGG1* promoter: GUS fusion. GUS staining revealed different levels of expression of *RGG1* in panicles at different developmental stages. As is shown in Figure 2a, the expression of *RGG1* gradually decreased with panicle development. It was also expressed in roots, with particularly strong staining in root tips (Fig. 2b). Additionally, GUS staining showed that *RGG1* was also abundantly expressed in leaves, sheath, nodes, stems, and spikelets (Fig. 2c-h). Moreover, The GUS results were in agreement with our quantitative reverse transcription-PCR (qPCR) analyses, which showed preferentially high expression of *RGG1* in young panicles, decreasing as development progressed (Fig. 2i). In addition, we detected *RGG1* transcripts in other tissues using qPCR including leaves, stems, nodes, sheathes, and roots (Fig. 2i). These data suggest that *RGG1* may play an important role in panicle and seed development.

To observe the subcellular localization of RGG1, both green fluorescent protein (GFP) and fusion protein (RGG1-GFP) driven by the CaMV 35S promoter were transiently expressed in rice protoplasts. Similar to the signal of GFP, RGG1-GFP were also detected in the plasma membrane, cytoplasm and nucleus (Fig. 2j). To verify the function of the predicted NLS at the N-terminus, we also transiently expressed a truncated protein, $RGG1_{\Delta NLS}$-GFP, in rice protoplasts. However, the fluorescent signal of $RGG1_{\Delta NLS}$-GFP showed the same distribution with RGG1-GFP, suggesting that the putative NLS domain may not be functional (Fig. S2).

Over-expression of *RGG1* resulted in stunted yield charcateristics in the Nipponbare rice variety

To elucidate the biological function of *RGG1*, the over-expression and knock-out vectors were generated and then transformed into Nipponbare (NIP) using an *Agrobacterium tumefaciens*-mediated method. We obtained several successful transformed lines were obtained, which were confirmed by qPCR and sequencing. We chose two over-expression (OE) and mutant lines each for further analysis (Fig. 3a, b).

The relative expression level of *RGG1* in two OE lines (OE1 and OE2) were detected. Compared to NIP, the expression level of *RGG1* increased by eight- and twelve-fold in OE1 and OE2, respectively (Fig. 3b). As a result, OE1 and OE2 transgenic lines showed a semi-dwarf phenotype at maturity (Fig. 3c). Further analysis showed that all internodes length of OE lines were shorter than those in NIP (Fig. S3a,b).

Additionally, we also quantified other yield components, such as panicle length (PL), tiller numbers per plant (TN), grain number per panicle (GN) and 1000-grain weight (TGW) (Fig. 3h, i, l, Table S1). Both PN and TN had no difference between NIP and the two OE lines (Fig. 3h, i). However, the TGW of OE1 and OE2 were decreased by 19.20% and 19.44%, respectively, compared to NIP (Fig.3l). Further analysis suggested that *RGG1* affects grain length and width, but has no influence on grain thickness (Fig. 3e-k). In particular, grain lengths in the OE lines was decreased by 7.41% and 10.17%, respectively, compared to that in NIP (Fig. 3j). As expected, OE1 and OE2 also exhibited decreased grain yield per plant (Fig.3m). Taken together, over-expression of *RGG1* can cause semi-dwarf height and shortened grain length.

Additionally, two knockout mutants of *RGG1* were generated using CRISPR/Cas9 system in the NIP background (Fig. 3a). Sequencing results showed that both mutants, NIP-*rgg1-1* and NIP-*rgg1-2* had large deletion in target site and destroyed proteins. However, the mutant plants of lines NIP-*rgg1-1* and NIP-*rgg1-2* did not show obvious phenotypes including related to plant height and other yield component traits (Fig. 3c-m). This may be due to the extremely low expression level of *RGG1*, which we observed in NIP (Fig. 3b). Whether or not there is gene redundancy in *RGG1* involved signal transduction needs further study.

Over-expression of *RGG1* in the Wunyunjing 30 results in similar phenotype

To investigate whether *RGG1* shows similar effects as in NIP mutants in a *qpe9-1* mutant background, we performed transformations of Wunyunjing 30 (WYJ30), a high-yield variety of rice that naturally lacks a functional *qpe9-1*, and we measured plant height and other yield-related traits at maturity. Both WYJ30-OE1 and WYJ30-OE2 lines showed reduced plant height and shortened panicle length compared to WT-WYJ30 (Fig. S4a-d, Table S2). Additionally, compared to WT-WYJ30, the grain length of the two OE lines was reduced by 3.29% and 3.42%, respectively (Fig. S4e). There was no significant difference for grain width between WYJ30 and OE lines (Fig. S4f). As a result, overexpressing *RGG1* caused decreased 1000-grain weight and grain yield in WYJ30 (Fig. S4g, h). These results suggest that the roles of *RGG1* in regulating plant height and grain length are independent of the status of *qPE9-1*. Pyramiding different Gγ encoding genes is possible to modulating grain size in rice.

We also applied the CRISPR/Cas9 in WYJ30 to obtain several homozygous mutants of *RGG1*. We identified one WYJ30-*rgg1-1* with a 4-bp deletion and another with a 1-bp insertion (Fig. S5). Both mutations caused a destroyed GGL domain in WYJ30-*rgg1-1* and WYJ30-*rgg1-2* (Fig. S5). We observed no changes in plant morphology and grain size between WT-WYJ30 and these two mutants (Table S2). Taken together, knockout of *RGG1* may have a little effect on rice growth and development.

RGG1 regulates grain size via affecting cell division

The spikelet hull has an important impact on gran size determination. Compared with WYJ30, both OE lines had shorter grain length and thinner grain width (Fig. 4a, b). Generally, organ size is determined by cell expansion and division. To clarify the grain size differences between WYJ30 and OE lines, histological cross-sections of the spikelet hulls were analyzed (Fig. 4c-e). As is shown in Fig 4d and e,

both OE lines had a significantly larger cell area and decreased cell number than those of WYJ30. Furthermore, the epidermal cells of WYJ30 and transgenic lines were analyzed using scanning electron microscopy (SEM) (Fig. 4f). No obvious cell length and cell width were found between WYJ30 and OE lines (Fig. 4g, h). However, the longitudinal cells of the OE lines were less than that in WYJ30 (Fig. 4i). Overall, these results suggest that overexpressing *RGG1* suppressed cell division in the spikelet hulls and consequently reduced smaller grain size.

RGG1 is involved in cytokinin biosynthesis

We performed a transcriptome analysis to investigate the possible molecular pathway of *RGG1* in young panicles of NIP, NIP- *rgg1-2*, and NIP-OE2 due to the significant influences of RGG1 on panicle elongation and grain length that we observed. Compared with NIP, a total of 1463 differentially expressed genes (DEGs) were detected in OE2, of which 690 genes were up-regulated and 773 genes were down-regulated (Fig. 5a). We detected many fewer DEGs between the *rgg1-2* mutant and WT-NIP compared to those between NIP-OE2 and WT-NIP.

The detected DEGs were involved in diverse biological processes and metabolic pathways (Fig. S6). Analysis of the DEGs using Gene ontology showed the most enrichment in biological processes. Additionally, analyses in KEGG revealed that the DEGs were enriched in the Zeatin biosynthesis pathway (Fig. 5b). In particular, a large number of the DEGs are associated with cytokinin biosynthesis (Fig. 5c). Notable, one gene, LOC_Os01g40630, encoding a cytokinin-activating enzyme LOG responsible for converting inactive cytokinin to biologically active forms, was down-regulated in young panicles of NIP-OE2 (Fig. 5c, d). The expression level of several cytokinin-related genes were also confirmed using qPCR assay (Fig. S7a-f). These results suggest that *RGG1* might be involved in the cytokinin regulatory pathway.

To test the hypothesis, we measured the concentration of cytokinin in young panicles (Fig. 5e-h). The total contents of two cytokinin precursors, including iPR and tZR, in OE lines were similar with those in NIP (Fig. 5e, f). However, the contents of active forms, iP and tZ, were significantly lower in the OE lines than that in NIP (Fig. 5g, h). NIP-OE2 accumulated higher tZR content than NIP may due to the inefficient converting ability (Fig. 3f). These results suggest that over-expression of *RGG1* reduced the efficiency of converting cytokinin precursors to active forms, possibly as a result of lower expression of *LOG*, or other genes in the cytokinin pathway.

RGG1 affects cytokinin signaling

Heterotrimeric GTP-binding proteins (G proteins) are involved in multiple signal transduction process and intracellular responses to stimuli in plants. We also investigated whether *RGG1* affects cytokinin signaling transduction in rice. Shoot and root elongation assays were conducted to test the sensitivity to different concentrations of 6-benzylaminopurine (6-BA) (Fig. 6a). The experiments revealed an altered growth curve for the *RGG1* overexpression lines when treated with 6-BA. At low concentration, the shoot length of NIP and two mutants were more seriously inhibited than OE1 and OE2 (Fig. 6b). The inhibition

of root elongation by cytokinin was also compared between NIP and transgenic lines (Fig. 6c). The results showed that two OE lines had a reduced sensitivity to 6-BA in the inhibitory effect on root elongation (Fig. 6c). All these results indicated that *RGG1* is involved in cytokinin biosynthesis and signaling transduction in rice.

Discussion

Grain size is one of the important agronomic traits affecting rice yield and quality. Although a complex regulatory gene network related to grain size has been proposed (Miao et al., 2019; Li and Li 2016), the crosstalks between Heterotrimeric G proteins and cytokinin regulatory pathway on grain size controlling are poorly known. In this study, we show that overexpression of *RGG1* resulted in decreased plant height and grain length (Fig. 2 and Fig. S4). Physiological measurement suggested that the active cytokinin content was lower in OE lines than that in NIP (Fig. 5). 6-BA treatment assay showed that *RGG1* is involved in cytokinin signaling transduction. Thus, our findings demonstrate that *RGG1* is involved in cytokinin biosynthesis and signaling to control grain size as well as plant height.

Phylogenetic analysis revealed that rice RGG1 is a type A Gγ protein. It contains a conserved GGL domain and a CaaX motif at the C-terminus that is characteristic of Gγ subunits that broadly occur among plants and animals and ensure proper membrane targeting (Pandey 2019). Therefore, RGG1 represents a canonical Gγ protein. Subcellular location result showed that RGG1 localizes to the plasma membrane, cytoplasm, and nucleus (Fig. 2j). Generally, Gα and Gβγ dimers perceive a stimulus at the surface of the cell along the membrane and then separate to transmit the signal to downstream effectors (Hildebrandt et al., 1984). Previous studies have shown that the RGB1, RGG1 and RGG2 localize to the plasma membrane (Kato et al., 2004). However, it is difficult to understand the roles of G proteins within the nucleus. In nuclei of mammalian cells, Gβγ heterodimers interact with a transcription factor, AP-1, and, thus, likely have a transcriptional regulatory role there (Chang et al., 2013; Robitaille et al., 2010). In rice, GS3-GFP and DEP1-GFP were detectable in the membrane and nucleus and function as cofactors of OsMADS1 in regulating grain size (Liu et al., 2018). More recently, the type B Gβ subunit, RGG2, was also found to be localized to plasma membrane, cytoplasm and nucleus (Miao et al., 2019). All of these results suggest that localization of G proteins, including RGG1, to the nucleus is associated with G protein signaling and is involved in transcriptional regulation in rice.

Our qPCR and GUS staining results showed that *RGG1* were constitutively expressed in diverse tissues, especially in panicles and spikelets (Fig. 2a-i). To investigate the roles that *RGG1* played in panicle development, we successfully generated *RGG1* knock-out and over-expression lines. Knock-out lines, *rgg1-1* and *rgg1-2* had no obviously different phenotypes compared to the NIP (Fig. 3, Table S1 and S2). One possible reason is that *RGG1* normally has a very low expression levels in rice (Fig. 3b). In *Arabidopsis*, *agg1* or *agg2* mutant and *agg1agg2* double mutant have no changes in rosette size, while triple *agg1agg2agg3* mutants show the reduction in rosette size (Thung et al., 2012). Therefore, another possible explanation is that there is gene redundancy in *RGG1* involved signal transduction. In contrast, the over-expression lines, OE1 and OE2, showed decreased plant height and panicle length as well as

small grains, all of which consist with results from a previous study (Liu et al., 2018). In contrast, Swain *et al* reported that increased expression of *RGG1* resulted in increased plant height and enhanced tolerance to salinity stress (Swain et al., 2017). Therefore, we evaluated the salinity stress tolerance using our transgenic lines in the background of NIP. The results revealed that seedlings of the OE lines did not show increased tolerance to salinity stress under treatments with 200 mM NaCl (Fig. S10). Thus, our results support a yield reduction and reduced plant height when *RGG1* is overexpressed, not increased height or increased salt tolerance.

We also over-expressed *RGG1* in the background of WYJ30, which contains a loss function allele *qpe9-1*. Similar phenotypes, including semi-dwarf plant architecture, shortened panicle length, decreased grain length, and overall lower yield production, were also observed in OE lines (Fig. S4, Table S2). Therefore, *RGG1* and *qPE9-1* may function differently in controlling grain size and grain yield characteristics, especially given that WYJ30 is a high-yield variety. Although the roles of Gβ and Gγ subunits in regulating grain size are well known, the mechanisms of G proteins meditated still remain poorly understood. For example, Sun *et al* reported that the Gγ subunit, *GS3*, may have no effect on regulating grain size by itself, while DEP1 and GGC2 compete with RGB1 to modulate grain size. Additionally, a previous study showed that G protein β and γ subunits could physically interact with the transcription factor, OsMADS1, to promote its transcriptional activity, thereby controlling grain morphology (Liu et al., 2018). Recently, we functional analyzed one gene, *RGG2*, and found that *RGG2* negatively regulate grain size via gibberellin pathway (Miao et al., 2019). These prior studies and our present results suggest that the mechanism of regulation of grain size by G proteins is likely very complicated. However, a more complete understanding of how G proteins operate to control grain size in rice is urgently needed to better manipulate size to meet global consumer demands.

To understand the possible regulatory pathway that *RGG1* meditates, we performed a transcriptome analysis using young panicles of NIP and transgenic plants. Results showed that many DEGs are associated with cytokinin biosynthesis (Fig. 5). In particular, one gene, *LOG*, showed significantly lower expression in the OE lines (Fig. 5C and Fig. S7b). *LOG* is responsible for converting cytokinin precursors to bioactive forms, and its mutant has a defect in inflorescence meristem development (Kurakawa et al., 2007). Cytokinins are adenine derivatives that play essential roles in regulating shoot meristem development (Hwang et al., 2012). However, the relationship between cytokinins and G proteins in mediating developmental processes in plants is poorly known. In *Arabidopsis*, in addition to the canonical Gα protein, there are three EXTRA-LARGE Gα-like PROTEINs (XLGs) that interact with U-box, PUB, E3 ligases, PUB2 and PUB4, and both the triple mutant *xlgs* and *pub2/4* double mutant showed defects in cytokinin response. Within the mutant lines, overexpression of *ARR10*, a positive cytokinin response regulator, partially rescued the defective phenotypes (Wang et al., 2017). Recently, Zhang *et al* reported that *qPE9-1*/*DEP1* positively regulates grain-filling via increasing auxin and cytokinin content in rice grains. Here, we revealed that the concentration of endogenous cytokinin was decreased in OE lines compared with that in NIP due to the decreased expression of genes encoding cytokinin biosynthesis enzymes. Cytokinin signaling comprises a classic two-step phosphorelay system where an initial signal is

transferred to a response regulator (Argueso et al., 2010; Hwang et al., 2012). Here, we also found *RGG1* is involved in cytokinin signal transduction based on a 6-BA treatment assay (Fig. 6a-c).

Overall, our findings along with prior work help to show the complicated crosstalk between G proteins and cytokinin. The critical nature of G proteins in plant development is highlighted by recent reports of knockouts of Gβ (*RGB1*) or Gγ (*RGG2*) in rice or Gβ (*ZmGB1*) in maize causing lethal phenotypes (Gao et al., 2019; Miao et al., 2019; Wu et al., 2020). This may be unsurprising given that G proteins probably mediate shoot meristem size through interaction with CLAVATA receptors (Bommert et al., 2013; Ishida et al., 2014; Wu et al., 2020) and may impact embryo formation via network between G proteins and cytokinin. We expect that further elucidating the interplay between cytokinin and G proteins will be beneficial for crop improvement via genetic engineering and molecular breeding.

Materials And Methods

Plant Materials and Growth Conditions

The wild type (Nipponbare and Wuyunjing30) and transgenic lines of the T_3 generation were used for phenotypic analyses. These materials were grown in experimental farm of Yangzhou University followed the normal agricultural practices. For analyses at the seedling stage, plants were grown in hydroponic culture in a growth chamber with a 12-h light (30℃) and 12-h dark (28℃) photoperiod and 70% humidity.

Homologous Detection and Phylogenetic Analysis

The sequences of the rice, *Arabidopsis* and maize Gγ proteins were obtained from NCBI (https://www.ncbi.nlm.nih.gov/). Multiple alignments were performed using Clustal X. Maximum likelihood (ML) and neighbor-joining (NJ) methods were adopt to analyze the phylogenesis using MEGA v7.0. The ML phylogenetic analyses were conducted with the following parameters: Jones-Taylor-Thornton (JTT) model, estimated proportion of invariable sites, 4 rate categories, estimated gamma distribution parameter, and optimized starting BIONJ tree. In addition, the JTT model was also employed for the construction of NJ trees. A total of 1000 non-parametric bootstrap samplings were carried out to estimate the support level for each internal branch for both the ML and NJ trees.

Vector Construction and Rice Transformation

To construct the *RGG1*-OE vector, the full length of coding sequence was amplified from Nipponbare cDNA and then inserted into the p1301Ubi vector. To generate pC1300-Cas9-g^{RGG1} mutants, we designed the target sequence in the first exon, the finally fragment was inserted into pC1300-Cas9 vector. The 2.0-kb promoter sequence of *RGG1* was cloned to drive the β-glucuronidase (GUS) gene and the promoter-GUS vector was transformed into Nipponbare. All these vectors were introduced into *Agrobacterium tumefaciens* strain EHA105 for subsequent transformation of Nipponbare (NIP) or Wuyunjing 30 (WYJ30). The homozygous T_2 generation plants were used for further analysis.

All primers used in this study are listed in Supplemental **Table S3**.

Histochemical GUS Staining and subcellular localization analysis

For GUS staining, positive transgenic plants were selected at different development stages using x-gluc kit (Real-Times (Beijing) Biotechnology Co. Ltd.). Leaves, node, sheath, stem, root, and young panicles of different stages were taken and then soaked in solution with x-gluc in 37℃ dark environment for one night. Then, samples were decolorized with absolute ethanol for observing.

For subcellular localization analysis, the full-length cDNA of *RGG1* gene was amplified and cloned into the pCAMBIA1300-221GFP vector generating a 35S::RGG1-GFP. The construct wad directly transformed into protoplasts of rice and the GFP signals were observed by confocal microscope (Leica). Relative primers are listed in Supplemental **Table S3**.

Evaluation of agronomic traits

Before harvested, several yield-related agronomic traits were measured including plant height, internode length, till numbers, and panicle length of main stem. For grain-related traits including grain length, grain width, and 1000-grain weight were measured after harvesting and stored at 37°C for one week. The total seeds of one plant taken out empty grain were weighed for grain yield per plant. Data statistic and sample *t-test* were analyzed using Excel (2016) software.

Histological analysis

Fresh young spikelet hulls of WYJ30 and WYJ30-OEs were taken and fixed in 2.5% glutaraldehyde for more than 24 h and then dehydrated through a graded series of alcohol-isoamyl acetate. Images of cross-section were taken on on a Zeiss Axioskop HBO 50 or a Leica MZFLIII fluorescence stereomicroscope. For glume cell observation, the outer surfaces of mature seeds were observed by scanning electron microscope (S-4800, Hitachi). Cell number and cell area in the outer parenchyma cell layer were measured using ImageJ software.

RNA extraction and qPCR

The total RNA was extracted using RNA extraction kit (Beijing Tiangen Biotechnology Co. Ltd.). High-quality RNA was used for generate cDNA using a FastQuant RT Kit (Beijing Tiangen Biotechnology Co. Ltd.). Gene expression level were analyzed using quantitative reverse transcription-PCR (qPCR). The rice *Actin* gene was used as internal control. The qPCR was carried out in a total volume of 20 μL, containing 2 μL of the cDNA, 10mM of each primer, 10 μL of 2×SYBR green PCR master mix, and 0.4 μL of 50´ROX Reference Dye 2 (Vazyme biotech Co. Ltd.) and performed on ABI ViiA7 real-time PCR system. Primers used for qPCR were listed in Supplemental Table S3.

Cytokinin measurement ant treatment

For measurement of cytokinin, young panicles of NIP and transgenic plants were collected in liquid nitrogen. The measurement of cytokinin was performed as previous described (Cai et al., 2014). For cytokinin treatment, one week old seedlings were grown in hydroponic medium and then treated with different concentration of 6-benzylaminopurine (6-BA). After one-week treatment, shoot and root length were measured for analyzing the response to cytokinin. For gene expression analysis, 10-d old seedlings were grown in hydroponic medium containing 10 Mm 6-BA. Leaves were taken every 2 hours for RNA extraction, the expression level of *OsRR9* was detected by qPCR.

RNA-sequencing analysis.

Young panicles of Nipponbare and transgenic lines were taken for total RNA extraction using Trizol reagent kit (Invitrogen, Carlsbad, CA, USA). Construction of the cDNA library and sequencing were performed at the Gene Denovo Biotechnology Co. (Guangzhou, China) using the Illumina HiSeq2500 (Illumina Inc., San Diego, CA, USA). The filtered clean reads were aligned to the rice Nipponbare reference genome and genes (http://rice.plantbiology.msu.edu/) using HISAT2. 2.4. RNAs differential expression analysis was performed by DESeq2.

Yeast two-hybrid Assay

To detect the interactions between RGG1 and RGB1, the full length and truncated sequence of *RGG1* were cloned pGADT7 vector, and the RGB1 was cloned into pGBKT7 vector. Yeast two-hybrid assays were performed according to the manufacturer's user manual. Primers used for qPCR were listed in Supplemental Table S3.

BiFC analysis

For BiFC assay, the coding sequence of RGG1 was cloned into pCAMBIA1300-35S-N-YFPn and the coding sequence of RGB1 was cloned into pCAMBIA1300-35S-N-YFPc vector. The plasmids were electroporated into *A. tumefaciens* (strain GV3101) and coinfiltrated into tobacco (*Nicotiana benthamiana*) leaves. After infiltration for 2-3 days, the GFP signals were observed by confocal microscope (Leica). Primers used for qPCR were listed in Supplemental Table S3.

Statistical analysis

Results are presented as mean±SD. Microsoft Excel 2016 was used for statistical tests. GraphPad Prism 8 was used for bar charts and line charts drawing. Significance levels were determined according to Student's *t*-test: $*P < 0.05$, $**P < 0.01$.

Declarations

Acknowledgements

We would like to thank all colleagues at the Jiangsu Academy of Agricultural Sciences and Yangzhou University for reading and participating in the discussions relating to the preparation of this manuscript.

Funding

This study was funded by the National Natural Science Foundation of China (31901525), the Natural Science Foundation of Jiangsu Province (BK20190255), the Jiangsu Province Key Research and Development Program (Modern Agriculture) Project (BE2019342-2), the Jiangsu Agricultural Science and Technology Innovation Fund (CX(18)2022).

Conflicts of interest

The authors declare no conflicts of interest.

Ethics Approval and Consent to Participate

Not applicable.

Consent for Publication

Not applicable

Availability of Data and Materials

The datasets supporting the conclusions of this article are included within the article and its additional files.

Author contributions

YJ, LGH, and ZY designed the experiments. TYJ, MJ wrote this paper and performed most of the experiments with the assistance of CZH, and JYJ. ZL, WJ, FFJ performed phenotype measurements. XY, LWQ, and WFQ constructed some vectors. TYJ and MJ contribute equally to this work.

References

Argueso CT, Raines T, Kieber JJ (2010) Cytokinin signaling and transcriptional networks. Curr Opin Plant Biol 13:533-539.

Ashikari M, Sakakibara H, Lin S, Yamamoto T, Takashi T, Nishimura A, Angeles ER, Qian Q, Kitano H, Matsuoka M (2005) Cytokinin oxidase regulates rice grain production. Science 309:741-745.

Blázquez M, Nelson D, Weijers D (2020) Evolution of plant hormone response pathways. Annu Rev Plant Biol:10.1146/annurev-arplant-050718-100309.

Bommert P, Je BI, Goldshmidt A, Jackson D (2013) The maize Galpha gene *COMPACT PLANT2* functions in CLAVATA signalling to control shoot meristem size. Nature 502:555-568.

Cai BD, Zhu JX, Gao Q, Luo D, Yuan BF, Feng YQ (2014) Rapid and high-throughput determination of endogenous cytokinins in *Oryza sativa* by bare Fe_3O_4 nanoparticles-based magnetic solid-phase extraction. J Chromatogr A 1340:146-150.

Chang C, Lee L, Yu D, Dao K, Bossuyt J, Bers D (2013) Acute β-adrenergic activation triggers nuclear import of histone deacetylase 5 and delays G(q)-induced transcriptional activation. The Journal of biological chemistry 288:192-204.

Gao S, Fang J, Xu F, Wang W, Sun X, Chu J, Cai B, Feng Y, Chu C (2014) Cytokinin oxidase/dehydrogenase4 integrates cytokinin and auxin signaling to control rice crown root formation. Plant Physiol 165:1035-1046.

Gao Y, Gu H, Leburu M, Li X, Wang Y, Sheng J, Fang H, Gu M, Liang G (2019) The heterotrimeric G protein β subunit RGB1 is required for seedling formation in rice. Rice 12:53.

Hildebrandt JD, Codina J, Risinger R, Birnbaumer L (1984) Identification of a gamma subunit associated with the adenylyl cyclase regulatory proteins Ns and Ni. J Biol Chem 259:2039-2042.

Huang X, Qian Q, Liu Z, Sun H, He S, Luo D, Xia G, Chu C, Li J, Fu X (2009) Natural variation at the *DEP1* locus enhances grain yield in rice. Nat Genet 41:494-497.

Hwang I, Sheen J, Muller B (2012) Cytokinin signaling networks. Annu Rev Plant Biol 63:353-380.

Ishida T, Tabata R, Yamada M, Aida M, Mitsumasu K, Fujiwara M, Yamaguchi K, Shigenobu S, Higuchi M, Tsuji H, Shimamoto K, Hasebe M, Fukuda H, Sawa S (2014) Heterotrimeric G proteins control stem cell proliferation through CLAVATA signaling in Arabidopsis. EMBO Rep 15:1202-1209.

Kato C, Mizutani T, Tamaki H, Kumagai H, Kamiya T, Hirobe A, Fujisawa Y, Kato H, Iwasaki Y (2004) Characterization of heterotrimeric G protein complexes in rice plasma membrane. Plant J 38:320-331.

Kurakawa T, Ueda N, Maekawa M, Kobayashi K, Kojima M, Nagato Y, Sakakibara H, Kyozuka J (2007) Direct control of shoot meristem activity by a cytokinin-activating enzyme. Nature 445:652-655.

Liu Q, Han R, Wu K, Zhang J, Ye Y, Wang S, Chen J, Pan Y, Li Q, Xu X, Zhou J, Tao D, Wu Y, Fu X (2018) G-protein betagamma subunits determine grain size through interaction with MADS-domain transcription factors in rice. Nat Commun 9:852.

Mao H, Sun S, Yao J, Wang C, Yu S, Xu C, Li X, Zhang Q (2010) Linking differential domain functions of the GS3 protein to natural variation of grain size in rice. Proc Natl Acad Sci U S A 107:19579-19584.

Miao J, Yang Z, Zhang D, Wang Y, Xu M, Zhou L, Wang J, Wu S, Yao Y, Du X, Gu F, Gong Z, Gu M, Liang G, Zhou Y (2019) Mutation of RGG2, which encodes a type B heterotrimeric G protein γ subunit, increases grain size and yield production in rice. Plant Biotech J 17:650-664.

Li N, Li Y (2016) Signaling pathways of seed size control in plants. Curr Opin Plant Biol 33:23-32.

Pandey S (2019) Heterotrimeric G-protein signaling in plants: conserved and novel mechanisms. Annu Rev Plant Biol 70:213-238.

Robitaille M, Gora S, Wang Y, Goupil E, Pétrin D, Del Duca D, Villeneuve L, Allen B, Laporte S, Bernard D, Hébert T (2010) Gbetagamma is a negative regulator of AP-1 mediated transcription. Cellular signalling 22:1254-1266.

Stahl Y, Simon R (2010) Plant primary meristems: shared functions and regulatory mechanisms. Curr Opin Plant Biol 13:53-58.

Sun H, Qian Q, Wu K, Luo J, Wang S, Zhang C, Ma Y, Liu Q, Huang X, Yuan Q, Han R, Zhao M, Dong G, Guo L, Zhu X, Gou Z, Wang W, Wu Y, Lin H, Fu X (2014) Heterotrimeric G proteins regulate nitrogen-use efficiency in rice. Nat Genet 46:652-656.

Sun S, Wang L, Mao H, Shao L, Li X, Xiao J, Ouyang Y, Zhang Q (2018) A G-protein pathway determines grain size in rice. Nat Commun 9:851.

Swain DM, Sahoo RK, Srivastava VK, Tripathy BC, Tuteja R, Tuteja N (2017) Function of heterotrimeric G-protein gamma subunit RGG1 in providing salinity stress tolerance in rice by elevating detoxification of ROS. Planta 245:367-383.

Thung L, Trusov Y, Chakravorty D, Botella JR (2012) Gγ1+Gγ2+Gγ3=Gβ: the search for heterotrimeric G-protein γ subunits in *Arabidopsis* is over. J Plant Physiol 169:542-545.

Ueguchi-Tanaka M, Fujisawa Y, Kobayashi M, Ashikari M, Iwasaki Y, Kitano H, Matsuoka M (2000) Rice dwarf mutant d1, which is defective in the alpha subunit of the heterotrimeric G protein, affects gibberellin signal transduction. Proceedings of the National Academy of Sciences of the United States of America 97:11638-11643.

Utsunomiya Y, Samejima C, Takayanagi Y, Izawa Y, Yoshida T, Sawada Y, Fujisawa Y, Kato H, Iwasaki Y (2011) Suppression of the rice heterotrimeric G protein beta-subunit gene, RGB1, causes dwarfism and browning of internodes and lamina joint regions. Plant J 67:907-916.

Wang L, Xu Y-Y, Ma Q-B, Li D, Xu Z-H, Chong K (2006) Heterotrimeric G protein α subunit is involved in rice brassinosteroid response. Cell Research:14-20.

Wang Y, Wu Y, Yu B, Yin Z, Xia Y (2017) EXTRA-LARGE G PROTEINs interact with E3 LIGases PUB4 and PUB2 and function in cytokinin and developmental processes. Plant Physiol 173:1235-1246.

Wu Q, Xu F, Liu L, Char SN, Ding Y, Je BI, Schmelz E, Yang B, Jackson D (2020) The maize heterotrimeric G protein beta subunit controls shoot meristem development and immune responses. Proc Natl Acad Sci U S A 117:1799-1805.

Xiao Y, Liu D, Zhang G, Gao S, Liu L, Xu F, Che R, Wang Y, Tong H, Chu C (2019) Big Grain3, encoding a purine permease, regulates grain size via modulating cytokinin transport in rice. J Integr Plant Biol 61:581-597.

Yu Y, Assmann SM (2015) The heterotrimeric G-protein beta subunit, AGB1, plays multiple roles in the Arabidopsis salinity response. Plant Cell Environ 38:2143-2156.

Zhang D, Zhang M, Zhou Y, Wang Y, Shen J, Chen H, Zhang L, Lü B, Liang G, Liang J (2019) The rice G protein γ subunit DEP1/qPE9-1 positively regulates grain-filling process by increasing auxin and cytokinin content in rice grains. Rice 12:91.

Zhang DP, Zhou Y, Yin JF, Yan XJ, Lin S, Xu WF, Baluska F, Wang YP, Xia YJ, Liang GH, Liang JS (2015) Rice G-protein subunits qPE9-1 and RGB1 play distinct roles in abscisic acid responses and drought adaptation. J Exp Bot 66:6371-6384.

Zhou Y, Zhu J, Li Z, Yi C, Liu J, Zhang H, Tang S, Gu M, Liang G (2009) Deletion in a quantitative trait gene qPE9-1 associated with panicle erectness improves plant architecture during rice domestication. Genetics 183:315-324.

Zong Y, Song Q, Li C, Jin S, Zhang D, Wang Y, Qiu J, Gao C (2018) Efficient C-to-T base editing in plants using a fusion of nCas9 and human APOBEC3A. Nature biotechnology:DOI: 10.1038/nbt.4261.

Figures

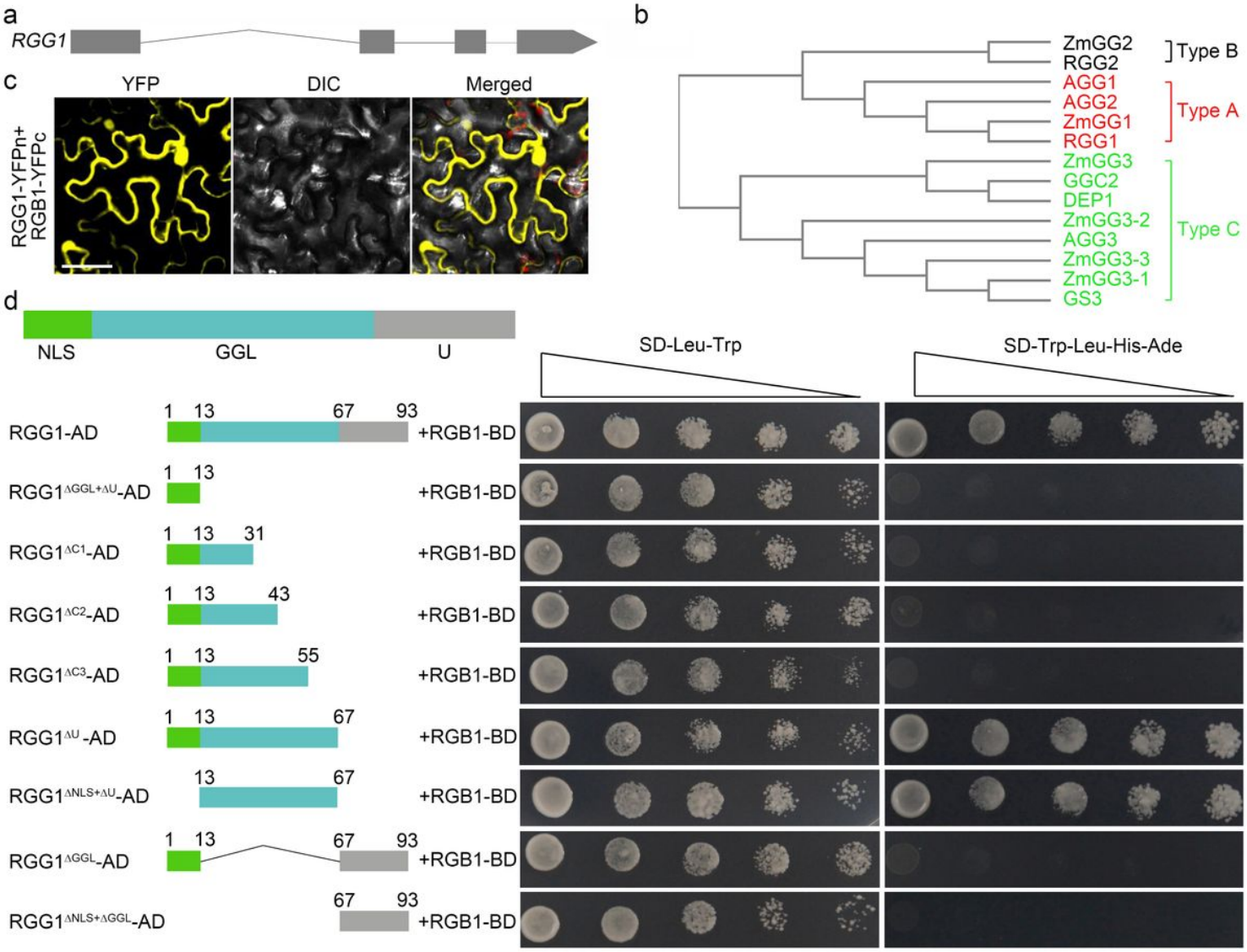

Figure 1

RGG1 encodes a type A Gγ subunit. (a) The gene structural of RGG1. (b) Phylogenetic tree of Gγ subunits from rice, Arabidopsis and maize. (c) Interaction between RGG1 and RGB1. Scale bars, 100 μm. (d) Yeast two-hybrid assay. In this assay, RGG1 is used as a prey (GAL4-AD, AD) due to its self-activating activity and RGB1 is used as a bait (GAL4-BD, BD). □□represents the deleted protein parts. The numbers show the different length of each truncated protein. NLS is the predicated nuclear localization signal. GGL is the G gamma-like domain. U represents the unknown domain.

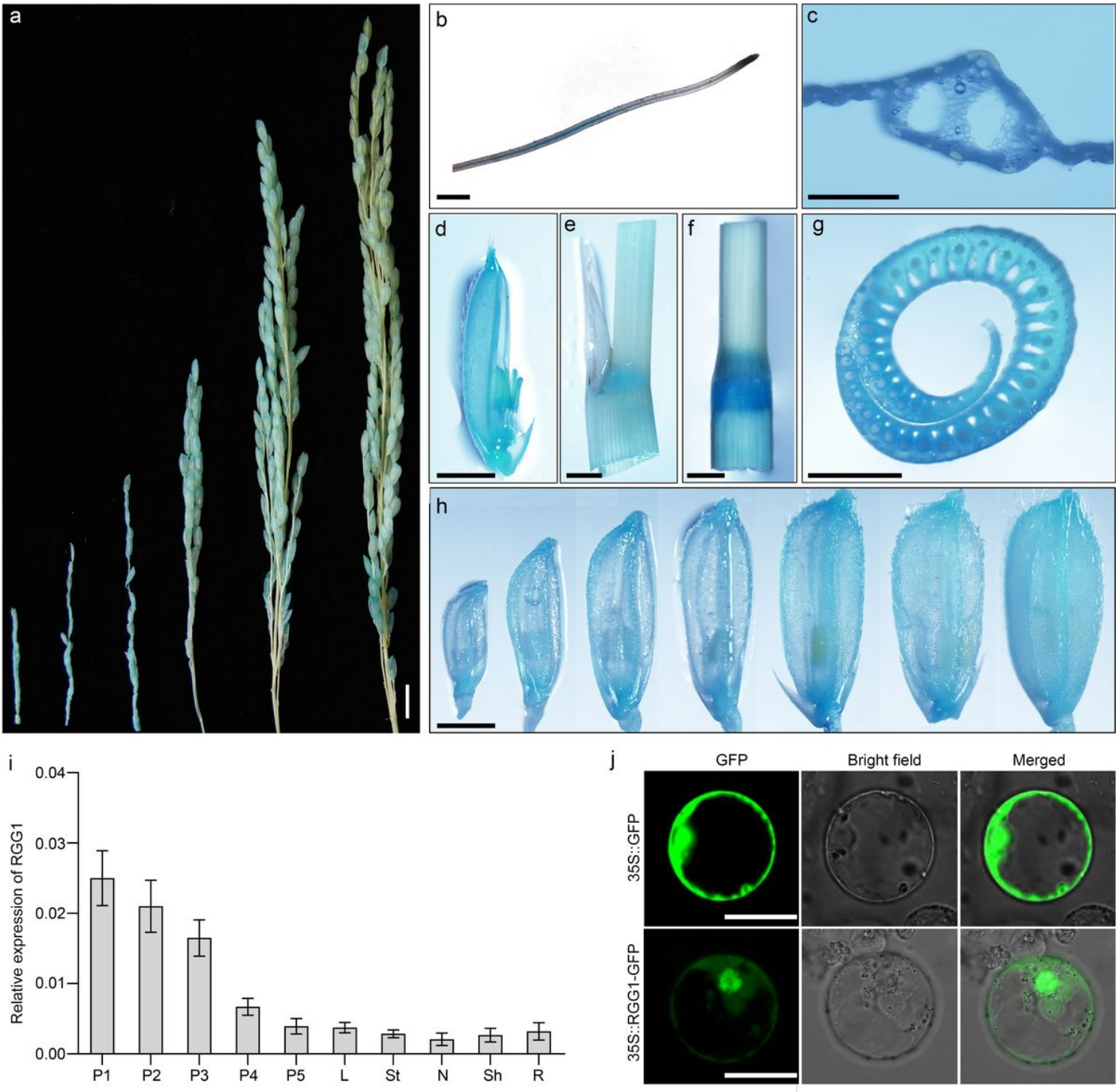

Figure 2

Molecular characterization of RGG1. (a) GUS activity in young panicles at different developmental stages. Scale bar, 1 cm. (b) GUS activity in root. Scale bar, 1 mm. (c) GUS activity in leaf. Scale bar, 50 μm. (d) GUS activity in spikelet. Scale bar, 2 mm. (e) GUS activity in sheath. Scale bar, 2 mm. (f) GUS activity in stem node. Scale bar, 2 mm. (g) GUS activity in node cross-section. Scale bar, 2 mm. (h) GUS activity in different developing spikelets. Scale bar, 2 mm. (i) RGG1 transcripts levels in different tissues. P1-P5, young panicles with the average length of about 3 cm, 6 cm, 10 cm, 13cm and >15 cm,

respectively. L, leaf. St, steam. N, node. Sh, sheath. R, root. (j) Subcellular location of RGG1 in rice protoplasts. Scale bar, 20 μm.

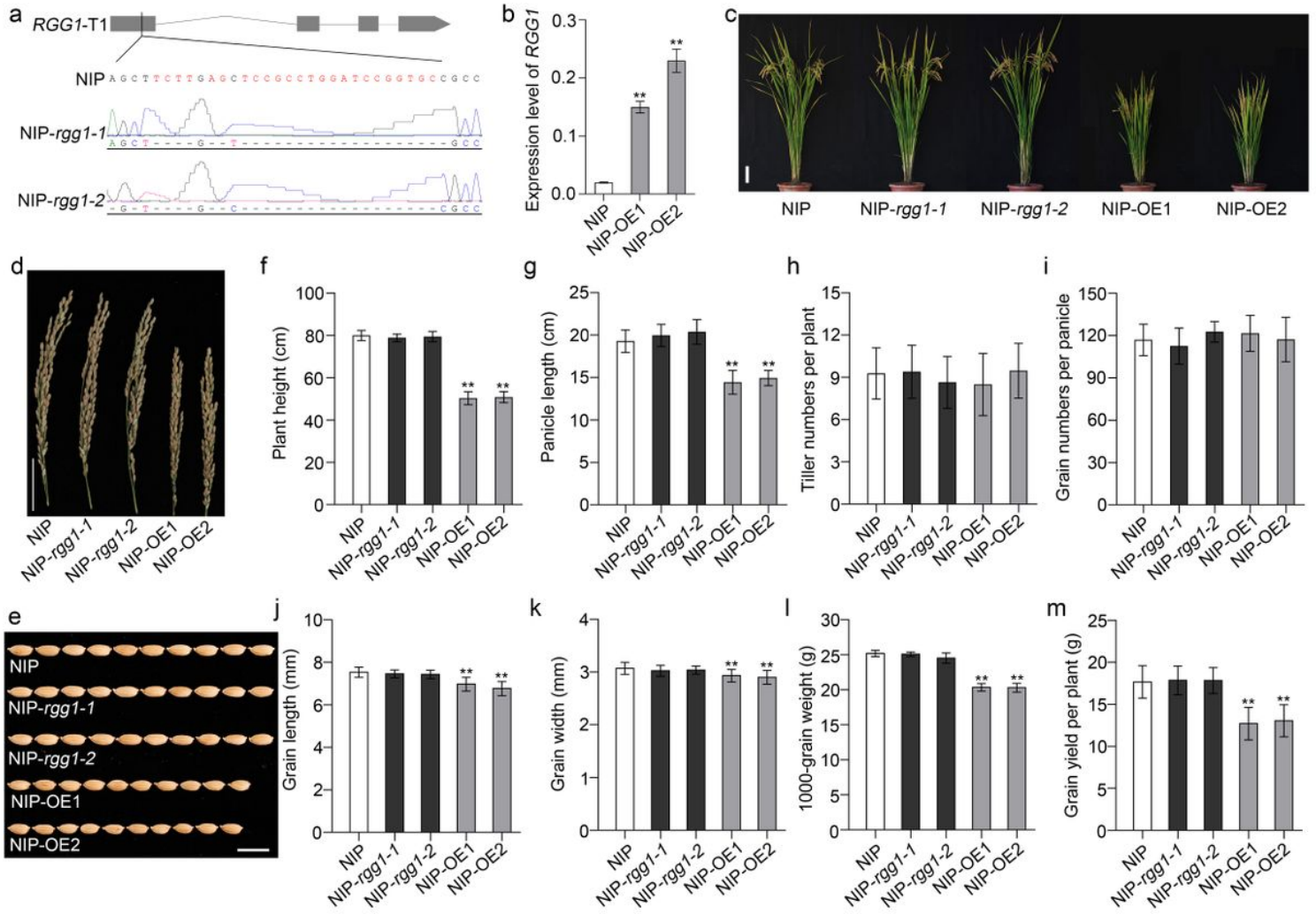

Figure 3

Overexpression of RGG1 has multiple effects on agronomic traits. (a) Targeted mutation of RGG1 generated two mutants (NIP-rgg1-1 and NIP-rgg1-2) using CRISPR/Cas9 system, which were confirmed by sequencing. (b) Relative expression levels of NIP and two RGG1 overexpression lines (NIP-OE1 and NIP-OE2). OsActin was selected as the internal control. (c) Plant morphology of NIP, NIP-rgg1-1, NIP-rgg1-2, NIP-OE1 and NIP-OE2 at mature stage. Scale bar, 10 cm. (d) Panicle phenotype of NIP, NIP-rgg1-1, NIP-rgg1-2, NIP-OE1 and NIP-OE2. Scale bar, 5 cm. (e) Grain size of NIP, NIP-rgg1-1, NIP-rgg1-2, NIP-OE1 and NIP-OE2. Scale bar, 1 cm. (f-m) Comparisons between NIP, mutants and OE lines with respect to (f) plant height; (g) panicle length; (h) till number per plant; (i) grain numbers per panicle; (j) grain length; (k) grain width; (l) 1000-grain weight; (m) grain yield per plant. The data are given as mean±SD (n≥20). Student's t-test: *P < 0.05, **P < 0.01.

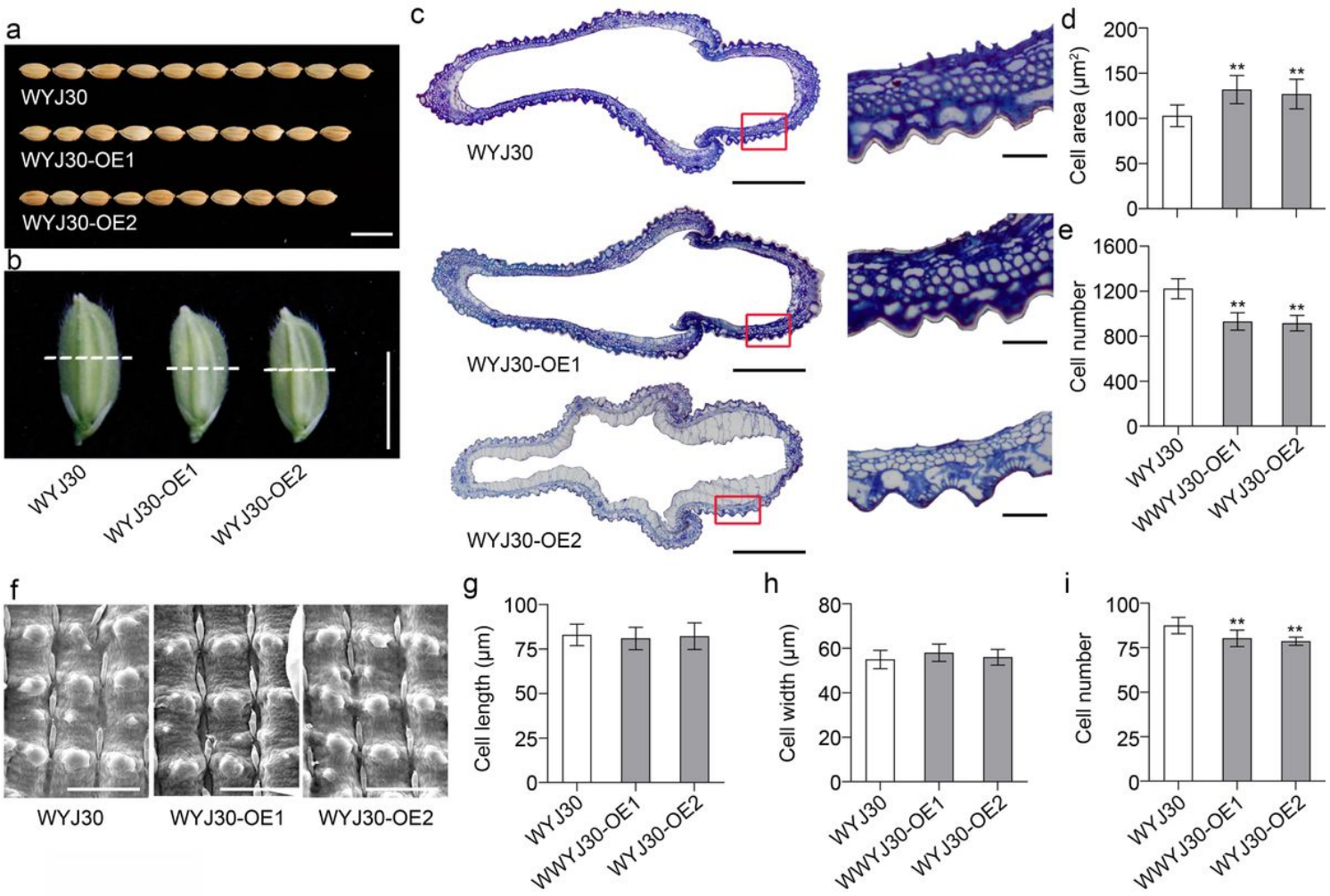

Figure 4

Histological comparison of the spikelet hulls between WYJ30 and two OE lines. (a) Grain size of WYJ30, WYJ30-OE1 and WYJ30-OE2. Scale bar, 1 cm. (b) Spikelet hulls of WYJ30, WYJ30-OE1 and WYJ30-OE2. Scale bar, 5 mm. (c) Cross-sections of the middle parts of the spikelet hulls (marked by white dashed lines in b) of WYJ30 and OE lines. Scale bar, 500 μm. Magnified views of the red boxed areas are listed on the right. Scale bar, 50 μm. (d) cell area and (e) cell number in the outer parenchyma layer of the spikelet hulls of WYJ30 and OE lines. (f) Scanning electron micrographs of the lemma cells of WYJ30 and OE lines. Scale bar, 100 μm. (g) cell length, (h) cell width and (i) cell number in longitude of WYJ30 and OE lines. The data are given as mean±SD (n≥15). Student's t-test: *P < 0.05, **P < 0.01.

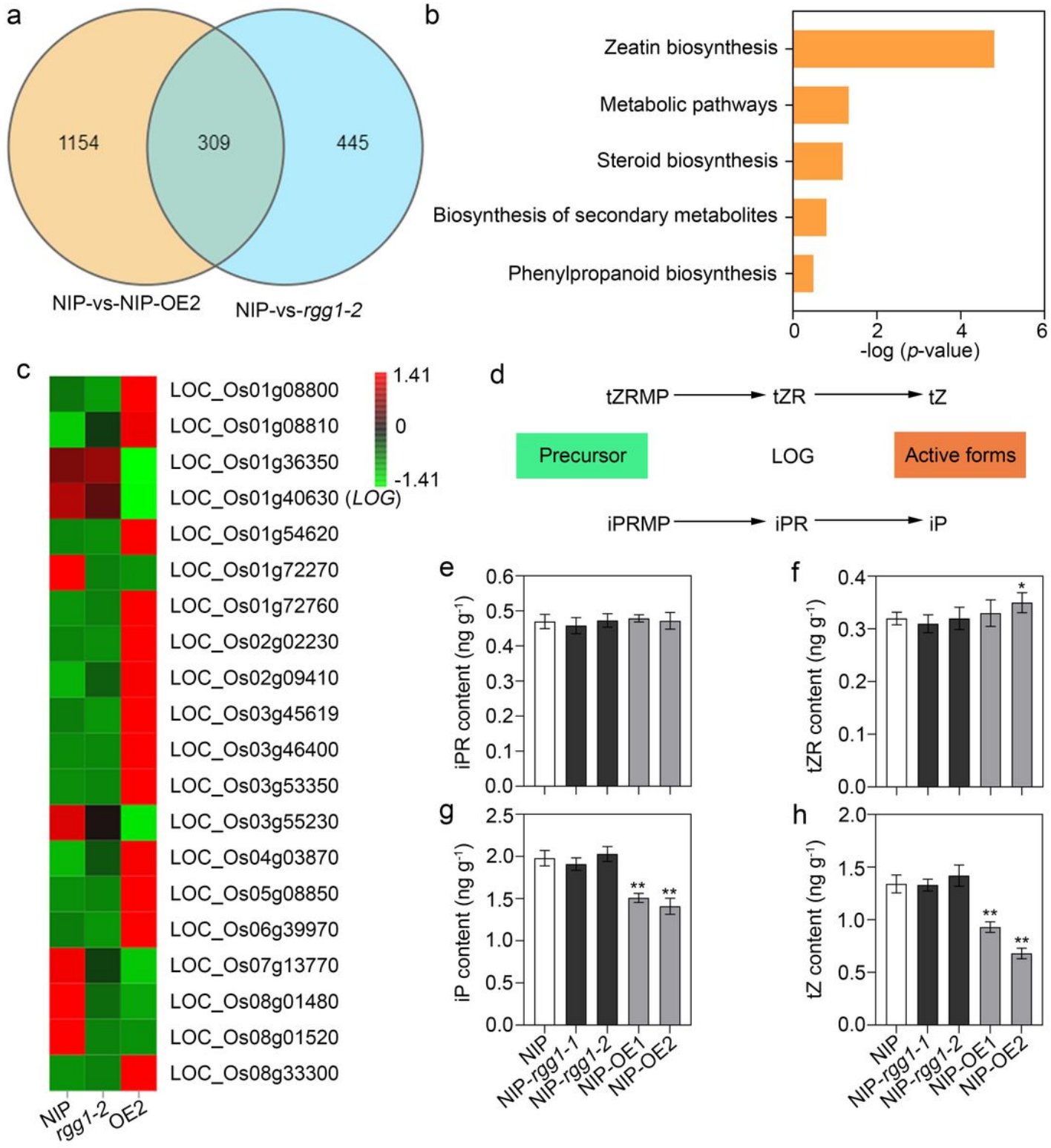

Figure 5

Transcriptome profiling in NIP, rgg1-2 and NIP-OE2. (a) Differentially expressed genes (DEGs) in young panciles of NIP and transgenic lines. (b) Kyoto encyclopedia of genes and genomes (KEGG) enrichment of DEGs. (c) Heat map of DEGs in cytokinin biosynthesis and regulation pathway. The different color in each box indicates the value of the Z-score. (d) The schematic of cytokinin biosynthesis pathway from precursor (tZRMP and iPRMP) to active forms (trans-zeatin, tZ and isopentenyladenine, iP). tZRMP, trans-

Zeatin riboside-5'-monophosphate. iPRMP, n6-(D2-isopenteny) adenine riboside momophosphate. tZ, trans-zeatin. iP, isopentenyladenine. (e) iPR content, (f) tZR content, (g) iP content and (h) tZ content in young panciles of NIP and transgenic lines (with three biological replicates). The data are given as mean±SD (n=3). Student's t-test: *P < 0.05, **P < 0.01.

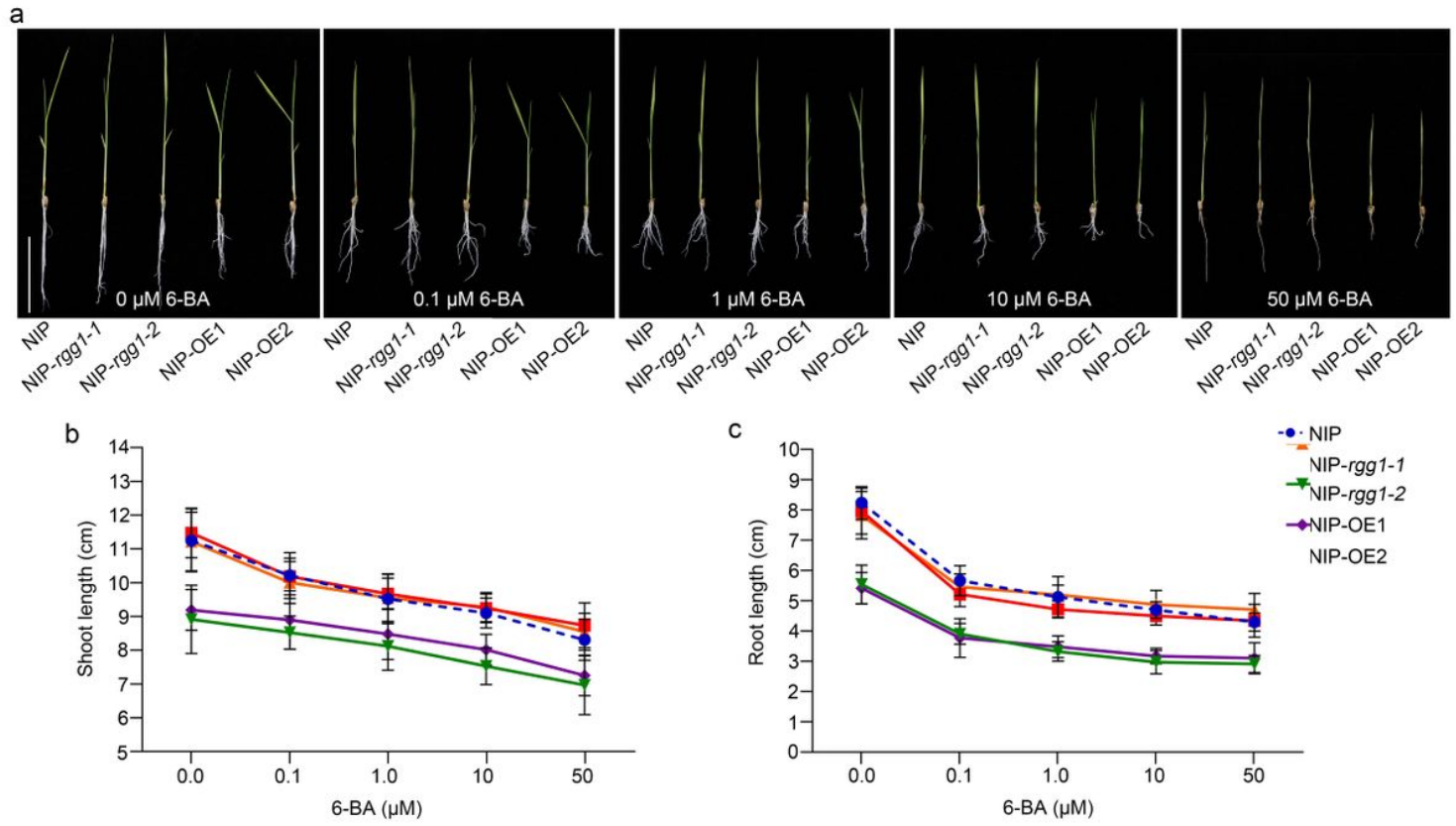

Figure 6

RGG1 is involved in cytokinin response. (a) Effect of different concentration of 6-BA treatment on growth of NIP and transgenic lines. Scale bar, 5 cm. (b) shoot and (c) root response to 6-BA treatment of NIP and transgenic lines (n≥12).

Supplementary Files

This is a list of supplementary files associated with this preprint. Click to download.

- supplementarymaterial.rar